MSK1 triggers the expression of the INK4AB/ARF locus in oncogene-induced senescence

Raphaël Culerrier[a], Maëlle Carraz[a,b], Carl Mann[c], and Malek Djabali[a,*]

[a]Université de Toulouse, UPS, LBCMCP, CNRS, F-31062 Toulouse, France; [b]Institut de Recherche pour le Développement, IRD, UMR 152 Pharma-DEV, Faculté des Sciences Pharmaceutiques, Université Toulouse 3, F-31062 Toulouse, France; [c]CEA, I2BC-CNRS UMR9198, Université de Paris-Saclay, F-91190 Gif-sur-Yvette, France

ABSTRACT The tumor suppressor proteins p15[INK4B], p16[INK4A], and p14[ARF], encoded by the INK4AB/ARF locus, are crucial regulators of cellular senescence. The locus is epigenetically silenced by the repressive Polycomb complexes in growing cells but is activated in response to oncogenic stress. Here we show that the mitogen- and stress-activated kinase (MSK1) is up-regulated after RAF1 oncogenic stress and that the phosphorylated (activated) form of MSK1 is significantly increased in the nucleus and recruited to the INK4AB/ARF locus. We show that MSK1 mediates histone H3S28 phosphorylation at the INK4AB/ARF locus and contributes to the rapid transcriptional activation of p15[INK4B] and p16[INK4A] in human cells despite the presence of the repressive H3K27me3 mark. Furthermore, we show that upon MSK1 depletion in oncogenic RAF1-expressing cells, H3S28ph presence at the INK4 locus and p15[INK4B] and p16[INK4A] expression are reduced. Finally, we show that H3S28-MSK–dependent phosphorylation functions in response to RAF1 signaling and that ERK and p38α contribute to MSK1 activation in oncogene-induced senescence.

INTRODUCTION

Cellular senescence is a stable form of cell-cycle arrest that is believed to limit the proliferative potential of premalignant cells (Serrano, 2007). Senescence can be triggered in different cell types in response to diverse forms of cellular damage or stress (for review, see Collado et al., 2007). The strong tumor-suppressive function of oncogene-induced cellular senescence (OIS) has been demonstrated in vivo in both humans and mouse models (Courtois-Cox et al., 2008). The INK4AB/ARF tumor suppressor locus is a master regulator of cellular senescence. In proliferating human and mouse cells, the locus is repressed by members of the Polycomb group (PcG; Bracken et al., 2007; Agherbi et al., 2009). The PRC2 complex initiates the repressive H3K27me3 chromatin mark, catalyzed by the histone methyltransferase activity of EZH2. This epigenetic mark is recognized by the maintenance complex PRC1 (Cao et al., 2002;

Cao and Zhang, 2004). It was demonstrated that the signaling pathway from oncogenic RAS-RAF counteracts INK4AB/ARF epigenetic Polycomb silencing in part by activating the H3K27 demethylase JMJD3. JMJD3 is recruited to the INK4AB/ARF locus and contributes to the transcriptional activation of p16[INK4A] in human diploid fibroblasts (Agger et al., 2009). The mitogen- and stress-activated protein kinases (MSK1 and MSK2), downstream targets of the p38 and extracellular signal-regulated kinase (ERK) pathways (Deak et al., 1998), are responsible for the histone H3 phosphorylation at serine 28 (H3S28ph) and serine 10 (H3S10p; Davie, 2003; Drobic et al., 2010). Studies show that an H3K27/H3S28 methyl/phospho switch mechanism regulates gene activation via PRC2 chromatin displacement during neuronal differentiation and mitogenic signaling (Gehani et al., 2010; Lau and Cheung, 2011a). Because Polycomb complexes negatively control the INK4AB/ARF locus in proliferating cells and are rapidly evicted from the locus when cells enter senescence, we wondered whether MSK1 participates in Polycomb complex eviction from the locus and thus contributes to the rapid expression of p15[INK4B] and p16[INK4A] in OIS.
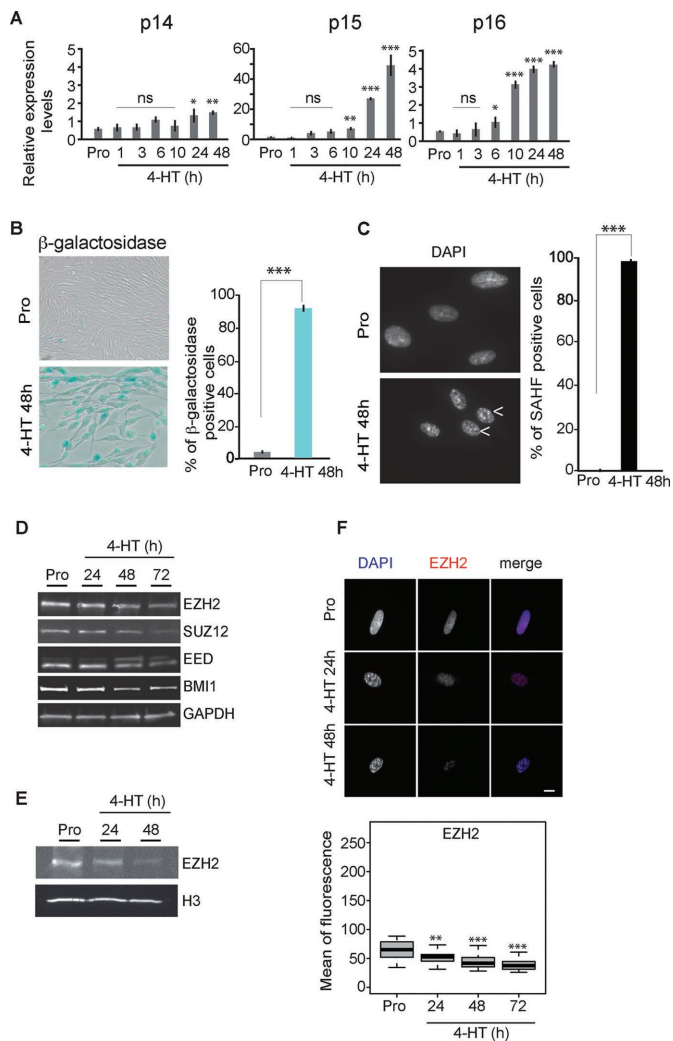
In the present study, we show that MSK1 is up-regulated and activated after oncogenic stress–induced senescence. MSK1 is recruited to the INK4AB/ARF locus, mediates H3S28 phosphorylation, and contributes to the rapid transcriptional activation of p15[INK4B] and p16[INK4A] in human cells through the displacement of Polycomb

FIGURE 1: Oncogene-induced senescence of WI-38h TERT RAF1-ER cells. (A) Expression levels of p14, p15[INK4B], and p16[INK4A] in WI38 hTERT RAF1-ER cells in proliferation (Pro) and at different time points (1, 3, 6, 10, 24, 48 h) after treatment with 20 nM 4-HT and determined by qRT-PCR. Mean and SD calculated from three independent biological experiments. Student's t test was used to determine statistical significance (*$p < 0.05$, **$p < 0.001$, ***$p < 0.0001$; ns, non significant). (B) SA-β-gal activity of proliferating WI-38hTERT/GFP-RAF1-ER cells (top) and WI-38hTERT/GFP-RAF1-ER cells induced into senescence by incubation with 4-HT for 2 d (bottom). Quantification of SA-β-gal–positive cells of WI38 hTERT RAF1-ER cells 48 h after 4-HT induction (right). Cells were plated at 2×10^4 /cm², induced for 48 h with 4-HT, stained for β-gal activity, and counted to calculate the average percentage β-Gal–positive cells. (C) Senescence-associated heterochromatin foci (SAHF). DAPI staining of WI-38hTERT RAF1-ER cells induced to senescence (4-HT, 48 h) and in proliferation (Pro). Quantification of SAHF-positive cells at 48 h after 4-HT treatment (***$p < 0.0001$). (D) Western blot analysis of PRC2 members (EZH2, SUZ12, EED) and PRC1 Bmi1 after 4-HT treatment (in hours); GAPDH served as a loading control. (E) Chromatin-associated EZH2 after 4-HT treatment; H3 served as a loading control. Quantification of these blots is given in Supplemental Figure S2B. (F) Top, immunofluorescence images for proliferating (Pro) and 4-HT induced (4-HT, 24 and 48 h) WI-38h TERT/GFP-RAF1-ER cells with EZH2 antibody (scale bars, 10 μm). Representative results from at least 20 fields observed in each of three independent experiments. Bottom, statistical analysis of EZH2 accumulation in cell nuclei in proliferation (Pro) and 24, 48, and 72 h after senescence induction. **$p < 0.001$ and *** $p < 0.0001$ by the Wilcoxon–Mann–Whitney test.

repressor complexes. We show that the H3S28-MSK–dependent phosphorylation functions in response to RAF1 signaling and that both ERK and p38α contribute to MSK1 activation in OIS.

RESULTS
A H3K27/H3S28 methyl/phospho switch mechanism regulates gene activation via PRC2 chromatin displacement during neuronal differentiation and mitogenic signaling (Gehani et al., 2010; Lau and Cheung, 2011a). MSK1 is responsible for the histone H3 phosphorylation at serine 28 (H3S28ph) and serine 10 (H3S10ph; Dyson et al., 2005). Because Polycomb complexes negatively control the INK4 locus in proliferating cells and are evicted from the locus when cells enter senescence, we wondered whether MSK1 participates in Polycomb eviction from INK4AB/ARF in OIS. To investigate a potential role of MSK1 in OIS, we took advantage of the WI-38hTERT human fibroblasts cell line, which expresses a conditional form of the RAF1 kinase (Jeanblanc et al., 2012). WI-38hTERT-RAF-ER cells rapidly undergo OIS and proliferation arrest accompanied by the rapid increased expression of the INK4A and INK4B genes encoding p15[INK4B] and p16[INK4A] (Figure 1A), which activate the Rb pathways (Takahashi et al., 2006). On RAF1 activation, cells present the senescence-specific marker senescence-associated β-galactosidase (SA-β-gal; Jeanblanc et al., 2012; Figure 1B). Senescence induction on 4-hydroxytamoxifen (4-HT) addition is very efficient, as shown by the rapid appearance of senescence-associated heterochromatin foci (Narita et al., 2003; Zhang et al., 2007; Figure 1C). This increased expression goes along with down-regulation of Polycomb repressor proteins and their eviction from the INK4 locus, as already described (Bracken et al., 2007; Agherbi et al., 2009; Figure 1D). Moreover Western blot analysis of chromatin-associated EZH2 shows that most of the protein is dissociated from the chromatin 48 h after senescence induction (Figure 1, E and F, and Supplemental Figure S2B). In addition, we examined through indirect immunofluorescence analysis the localization of endogenous EZH2. On induction of WI-38hTERT-RAF-ER cells, we observe a significant reduction of the nuclear pool of EZH2 at 24, 48, and 72 h after 4-HT treatment (Figure 1F).

MSK1 is activated during RAF1-induced cell senescence (OIS)
Quantitative real-time PCR (qRT-PCR) analysis establishes that MSK1 transcript is accumulated as soon as 24 h after senescence induction in 4-HT–treated cells (Figure 2A). Accordingly, Western blot and indirect immunofluorescence analysis show that indeed MSK1 significantly accumulates in RAF1-induced senescent cells 24 and 48 h after 4-HT induction (Figure 2, B and C). MSK1 activity requires phosphorylation of Ser-376 and Thr-581 (McCoy et al., 2005). To establish the kinetics of MSK1 phosphorylation, we stimulated RAF1 cells with 4-HT (Figure 2B). Subsequently we analyzed total cell lysates for MSK1 phosphorylation using a specific antibody for Ser-376 phosphorylation. In nonstimulated controls (time point 0 h), basal MSK1 phosphorylation is low, but MSK1 phosphorylation robustly increased 6 h after RAF1 induction and was maintained 48 h after induction in fully senescent cells (Figure 2B). In addition, indirect immunofluorescence analysis revealed that p-MSK1 was significantly enriched in the nucleus of 4-HT–induced cells (Figure 2D). This enrichment correlates with the significant increase of H3S28 phosphorylation observed in the nucleus of the senescent cells (Figure 2D, bottom). Taken together, these data suggest a potential function of MSK1 in OIS. To confirm that these results were not unique to RAF1-induced lung fibroblasts, we tested a second model of OIS using human BJ cells that were induced to enter senescence via a doxycycline-inducible form of the BRAFV600E oncogene (diBRAF). This system has been used in a well-established example
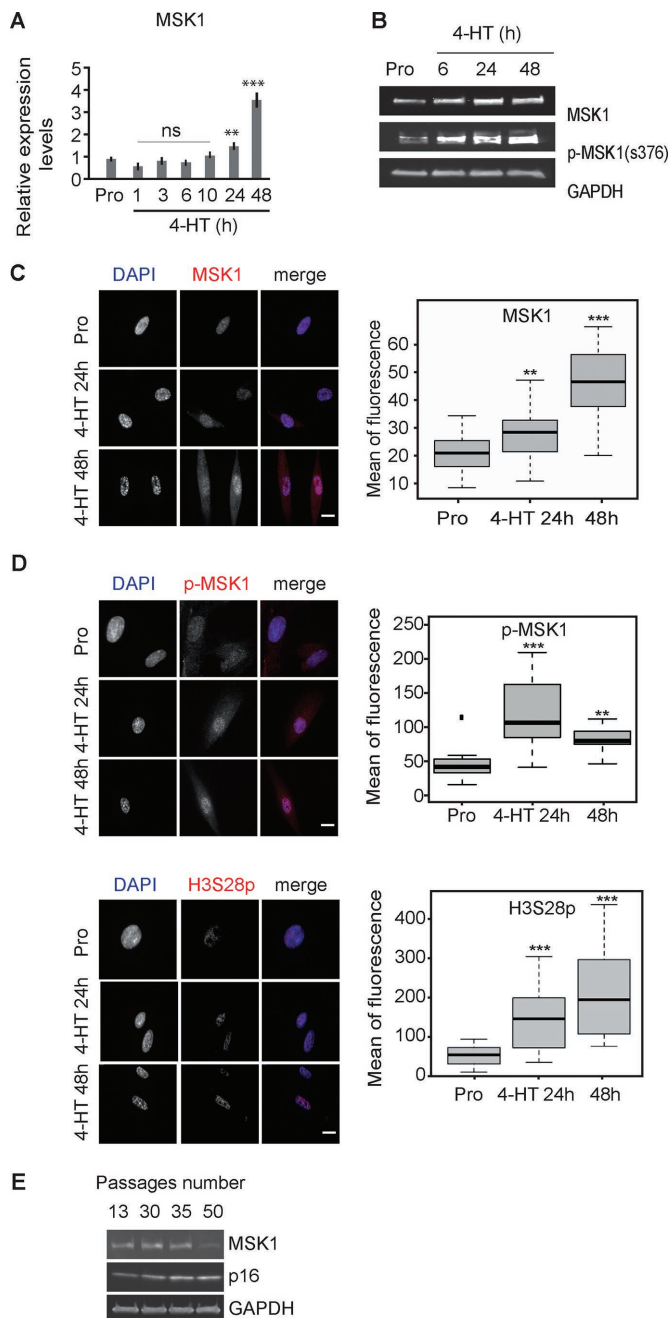
FIGURE 2: MSK1 is overexpressed and activated in OIS.
(A) Expression levels determined by qRT-PCR of MSK1 in WI-38h
TERT RAF1-ER cells in proliferation (Pro) and at different time points
(1, 3, 6, 10, 24, 48 h) after 4-HT treatment. Mean and SD are from
three independent experiments. Student's t test was used to
determine statistical significance (**$p < 0.001$, ***$p < 0.0001$).
(B) Immunoblot analysis of levels of MSK1 and p-MSK1 (Ser-376) in
whole-cell extracts prepared from WI-38h TERT/GFP-RAF1-ER cells
treated with 4-HT for the indicated number of hours. GAPDH was
used as a loading control. (C) Immunofluorescence images of
proliferating (Pro) and 4-HT–induced (4-HT 24 and 48 h) WI-38h TERT/
GFP-RAF1-ER cells with MSK1 antibody (scale bar, 10 μm). The results
are representative of those from at least 20 fields observed in each of
three independent experiments. (D) Left, immunofluorescence images
of proliferating (Pro) and 4-HT–induced (4-HT 24 and 48 h) WI-38h
TERT/GFP-RAF1-ER cells with p-MSK1 and H3S28ph antibodies (scale
bar, 10 μm). The results are representative of those from at least 20
fields observed in each of three independent experiments. Right,

statistical analysis of MSK1, p-MSK1, and H3S28ph accumulation in
cell nuclei in proliferation (Pro) and 24 and 48 h after senescence
induction (**$p < 0.001$ and ***$p < 0.0001$ by the Wilcoxon–Mann–
Whitney test). (E) Western blot analysis of MSK1 and p16 levels in
WI-38h wild-type cells passaged until replicative senescence (p50).

of in vivo OIS (Michaloglou *et al.*, 2005). As with our WI38-RAF1
analysis, we examined the expression of INK4 genes, Polycomb
(EZH2), and MSK1 after BRAFV600E induction and demonstrate
that in these cells, MSK1 is strongly up-regulated and the Polycomb
gene EZH2 is down-regulated (Supplemental Figure S1A). In addi-
tion, we monitored the expression of MSK1 in WI-38h wild-type cells
passaged until replicative senescence. MSK1 is overexpressed in
presenescent cells (p30 and p35), and this overexpression correlates
with overexpression of p16 at the same passages (Figure 2E). How-
ever, we observe a down-regulation of MSK1 in fully senescent cells
(p50), indicating that the function of MSK1 might not be required in
replicative senescence when cells are fully senescent.

H3K27me3/S28 phosphorylation correlates with a loss of PcG protein binding and the activation of INK4 genes

Phosphorylation of H3 on serine residues (S10 and S28) can be in-
duced by several signaling pathways and is associated with tran-
scriptional activation of diverse stimulus-responsive genes (Drobic
et al., 2010; Perez-Cadahia *et al.*, 2011). We sought to test the pos-
sibility that the previously reported H3K27/H3S28 methyl/phospho
switch mechanism (Gehani *et al.*, 2010; Lau and Cheung, 2011b)
could act at the INK4 locus to regulate the PRC2-EZH2 displace-
ment during OIS. To test this hypothesis, we performed chromatin
immunoprecipitation (ChIP) experiments at the INK4AB/Arf locus in
proliferating and senescent WI38-RAF1 cells using specific antibod-
ies against H3K27me3, H3K27Ac, H3S28ph, Polycomb EZH2, and
the activated form of MSK1 (p-MSK1(ser376)). ChIP experiments us-
ing an antibody against H3S28ph demonstrate that this mark is not
detected at the locus in proliferating cells, whereas the Polycomb
repressive mark H3K27me3 and the PRC2 member EZH2 are pres-
ent, as previously demonstrated (Bracken *et al.*, 2007; Agherbi
et al., 2009). However, the phosphorylation of H3S28 is robustly de-
tected at both p15[INK4B] and p16[INK4A] promoters and all over the
INK4 locus 24 h after 4-HT RAF1 induction. Surprisingly, the repres-
sive mark H3K27me3 is still strongly detected at the locus 24 h after
induction, although the PRC2 member EZH2 has been evicted from
the locus (Figure 3). Given that we detect H3K27me3 and the
H3S28ph mark 24 h after 4-HT induction, this indicates that the an-
tibody we used in our study efficiently recognized the H3K27me3
mark, even in the presence of the adjacent H3S28ph mark (Gehani
et al., 2010). This also indicates that the previously identified H3K27
demethylase JMJD3, whose expression is induced by OIS (unpub-
lished data) is not yet active at the INK4 locus 24 h after oncogene
induction (Agger *et al.*, 2009). Moreover, our results show that de-
spite the presence of the H3K27me3 repressive mark at 24 h after
induction, INK4 gene transcription is active since both p16[INK4A] and
p15[INK4B] are strongly expressed 10 and 24 h after 4-HT induction
(increase of 8- and 25-fold, respectively; Figure 1A). ChIP analysis
further show that the H3K27me3 mark is finally lost 48 h after 4-HT
induction (Figure 3B). Loss of H3K27me3 in the activation of Poly-
comb-regulated genes is frequently associated with concomitant
gain in H3K27 acetylation (Pasini *et al.*, 2010). Therefore we also
examined by ChIP the level of H3K27Ac at the INK4 locus after OIS
induction. In proliferating cells and 24 h after OIS induction, the
level of H3K27 acetylation is low all over the locus. In contrast, we
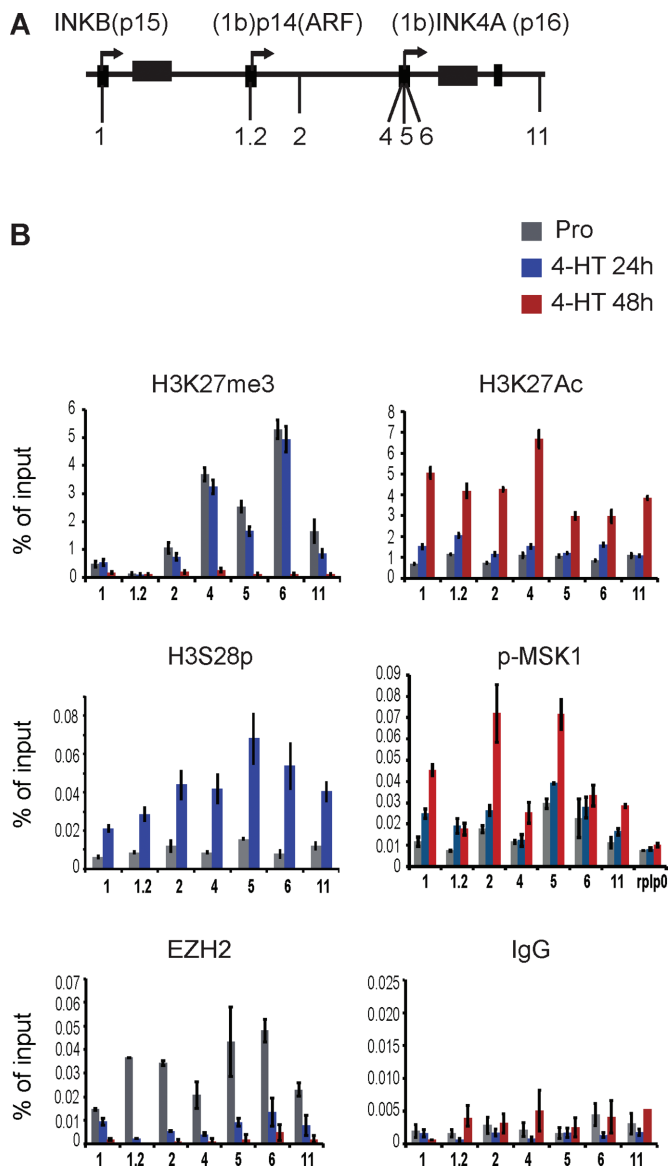
FIGURE 3: MSK1-dependent H3S28 phosphorylation affects PRC2-EZH2 chromatin displacement from the INK4 locus. (A) Schematic representation of the INK4AB/p14^{ARF} locus, showing the localization of the primer pairs used in the ChIP experiments performed in WI-38h TERT RAF1-ER cells. (B) ChIP at the INK4AB/ARF locus. ChIP analysis was performed on chromatin prepared from WI-38h TERT RAF1-ER proliferating cells (Pro) or induced to senescence for 24 and 48 h. Antibodies are listed above the graphs. The precipitated DNA fragments were subjected to qRT-PCR analysis with selected primers amplifying regions of the INK4AB/p14^{ARF} locus. General IgG was used as a negative control. The RPLP0 (gene ID: NM_001002) served as a negative control in p-MSK1 ChIP experiments. The values are shown as percentage of input. Data represent the average of three independent biological experiments and are expressed as means ± SD. Statistical analysis of the ChIP experiments is given in Supplemental Table S2.

observe a strong increase of H3K27 acetylation 48 h after OIS induction (Figure 3B). This correlates with complete loss of H3K27me3 at 48 h after induction and full expression of p15 and p16 (Figure 2A). Nevertheless, the significant induction of transcription of both p15^{INK4B} and p16^{INK4A} observed at 10 and 24 h after 4-HT induction was not correlated with H3K27Ac enrichment at the locus.

We next wanted to address whether MSK1 is recruited to the promoters of the INK4 genes. Of interest, ChIP analysis for p-MSK1 showed that this kinase seems to be prebound at the promoter of p16^{INK4A} in proliferating cells. MSK1 accumulation is significantly enriched at primers 1, 2, and 4–6 compared with the negative control primers for the RPLP0 gene (Supplemental Table S2), and, in addition, its amount increases significantly 24 and 48 h after RAF1 senescence induction (Figure 3B). Nevertheless, the Polycomb protein EZH2 is no longer detected at the locus 24 h after RAF1 induction. This suggests that the binding of Polycomb proteins is compromised by the phosphorylation of adjacent Ser-28 on H3 at the INK4AB locus (Gehani et al., 2010). Taken together, these results suggest that displacement of the PRC2-EZH2 complex from the INK4AB locus is regulated by an H3K27me3/H3S28ph switch via MSK1 recruitment onto chromatin.

MSK1 is required for INK4 gene early expression in OIS and is regulated by the ERK and p38α pathways

To directly assess MSK1 function in the expression of the INK4 locus in OIS, we performed loss-of-function experiments in which we transiently transfected WI-38hTERT-RAF1-ER cells with small interfering RNAs (siRNAs) targeting MSK1 48 h before inducing OIS by adding 4-HT. Western blot and qRT-PCR analysis show that MSK1 depletion is complete 48 h after siRNA transfection and that the activation of the ERK pathway after RAF1 induction is not affected by the siMSK1 transfection (Figures 4, A–C, and Supplemental Figure S1). qRT-PCR analysis revealed that the depletion of MSK1 strongly inhibits the expression of p15^{Ink4B} and p16^{INK4A} (Figure 4A and Supplemental Figure S1) 24 h after 4-HT treatment. Accordingly, Western blot analysis confirms that the level of the protein is also reduced upon MSK1 depletion and that both p-p38 and p-ERK are induced in MSK1-depleted cells (Figure 4B). Next we wanted to determine whether MSK1 is required for senescence phenotype induction and monitored the β-gal activity in cells induced to senescence and treated to knock out MSK1 expression. As shown in Figure 4C, β-gal activity is strongly impaired in MSK1-knockout cells 24 h after 4-HT induction compared with siNS control and nontransfected cells. However, β-gal activity is detected in 50% of MSK1-depleted cells 48 h after 4-HT induction, indicating that MSK1 could be mainly required for the induction of p15 and p16 and therefore senescence.

Finally, ChIP analysis in MSK1-depleted and 4-HT–induced cells show that the H3S28ph mark is significantly reduced at the locus, indicating that H3S28 phosphorylation at the INK4 locus is due to MSK1 kinase activity, and this suggests that the H3S28 phosphorylation is sufficient to permit the early expression of the INK4 genes after an oncogenic stress (Figure 4D).

Finally, we wanted to determine whether the overexpression of MSK1 was sufficient to induce senescence. Therefore we transfected WI-38hTERT-RAF1-ER cells with a pCMV5-Flag–wild-type MSK1 construct (Deak et al., 1998) with an empty control vector or left untransfected. We monitored the β-gal activity of these cells 48 h after transfection. As seen in Supplemental Figure S2A, the transfection of MSK1 does not induce senescence, as the number of β-gal–positive cells is not increased after MSK1 transfection. In addition, in both treated and transfected cells (4-HT + MSK1), the number of β-gal–positive cells is similar to that in control (4-HT), indicating that overexpression of MSK1 has no effect on senescence maintenance.

MSK1 activity is tightly regulated in cells, and its activation requires phosphorylation by either ERK1/2 or p38α (Deak et al., 1998). p38α is a member of the mitogen-activated protein kinase (MAPK) family of signaling molecules. It was demonstrated that oncogenic
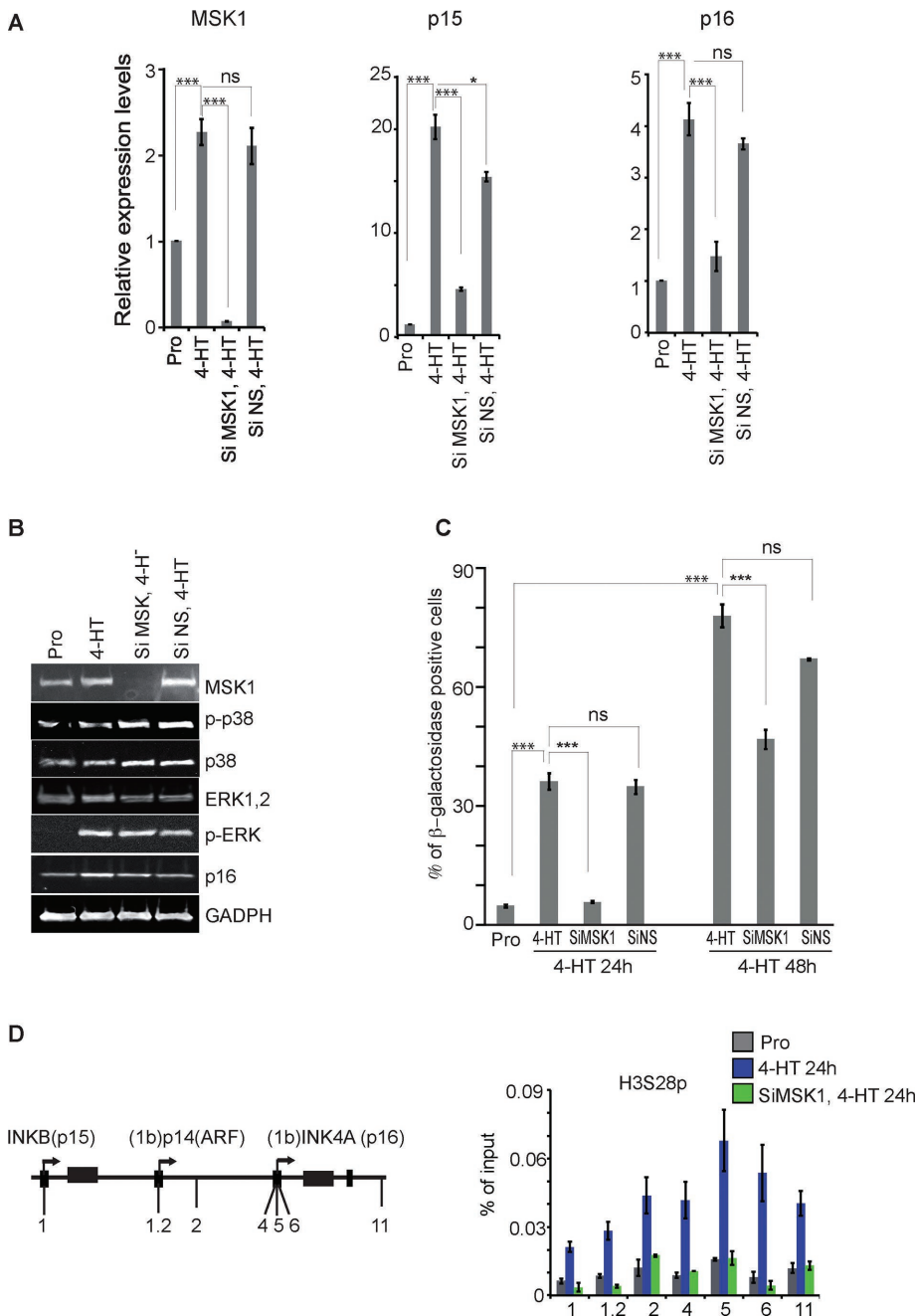
FIGURE 4: siRNA-mediated depletion of MSK1 inhibits oncogene-induced expression of p16[INK4A] and p15[INK4B]. (A) qRT-PCR analysis of p15[INK4B] and p16[INK4A] expression of WI-38h TERT-RAF-ER cells in siMSK1- and 4-HT–treated cells. Data represent the average of three independent biological experiments and are expressed as means ± SD. Student's *t* test was used to determine statistical significance (**p < 0.001, ***p < 0.0001; ns, nonsignificant). (B) Western blot analysis of MSK1, p-ERK, ERK, p38, p-p38, and p16[INK4A] in WI-38hTERT-RAF-ER siMSK1- and 4-HT–treated cells. (C) A β-gal assay in siMSK1- and 4-HT–treated cells 24 and 48 h after induction. Student's *t* test was used to determine statistical significance (*p < 0.05, ***p < 0.0001; ns, nonsignificant). (D) Left, schematic representation of the INK4AB/p14[ARF] locus, showing the localization of the primer pairs used in the ChIP experiments. Right, ChIP analysis was performed on chromatin prepared from siMSK1- and 4-HT–treated cells 24 h after 4-HT RAF1 induction using H3S28 phosphorylated (H3S28ph) antibody. General IgG was used as a negative control. The values are shown as percentage of the input. Data represent the average of three independent biological experiments and are expressed as means ± SD. Statistical analysis of the ChIP experiments are given in Supplemental Table S2.

ras induces senescence through the activation of the MAPK kinase-ERK pathway and the MKK3/6-p38 pathway in primary human fibroblasts (Wang *et al.*, 2002). Western blot analysis demonstrates that both p-ERK (Figure 4A) and p-p38 (Figure 5A) are activated after RAF1 induction. To evaluate the relative involvement of p38 and ERK in the activation of MSK1 and induction of p15[INK4B] and p16[INK4A] in RAF1 OIS, we took advantage of the SB203580 and PD98059 chemical inhibitors of p38 and ERK, respectively. Western blot analysis of inhibitor-treated cells showed that MSK1 fails to be phosphorylated at Ser-376 when treated by either SB203580 or PD98059, demonstrating that the activation of MSK1 depends on both p38 and ERK in RAF1 OIS (Figure 5C). Moreover, treatment of cells with SB20358 or PD98059 before activation of RAF1 by 4-HT strongly inhibits the expression of p15[INK4B] and partially blocks p16[INK4A] expression (Figure 5, B and C), demonstrating that p38- and ERK-dependent MSK1 activation is required for rapid activation of the INK4 locus in OIS. Finally, to confirm that the inhibition of transcription of p15[INK4B] and p16[INK4A] is due to MSK1/H3S28ph inhibition, we performed a ChIP analysis in PD98059-treated cells (Figure 5D). We showed, using an antibody against H3S28ph, that this mark is lost at the locus in PD98059-treated cells, demonstrating that the inhibition of the ERK pathway blocks MSK1-dependent H3S28 phosphorylation at the INK4 locus and therefore restrains the induction of expression of p15[INK4B] and p16[INK4A].

DISCUSSION

In previous work, we and others demonstrated that the epigenetic regulation of the INK4AB/ARF locus is achieved through the Polycomb repressive complexes PRC1 and 2 (Bracken *et al.*, 2007; Agherbi *et al.*, 2009). The PRC2 complex establishes the repressive H3K27me3 chromatin mark, catalyzed by the histone methyltransferase activity of EZH2. This epigenetic mark is recognized by the PRC1 maintenance complex, establishing the stable repression of the locus. The INK4AB/ARF locus is maintained repressed in normal proliferating conditions but is quickly activated in stress conditions. Therefore stimuli that trigger its induction have to modify the epigenetic profile of the locus to eliminate the Polycomb complexes and their repressive marks. It was demonstrated that the level of EZH2 is decreased during replicative senescence and OIS (Bracken *et al.*, 2007). In addition, the H3K27
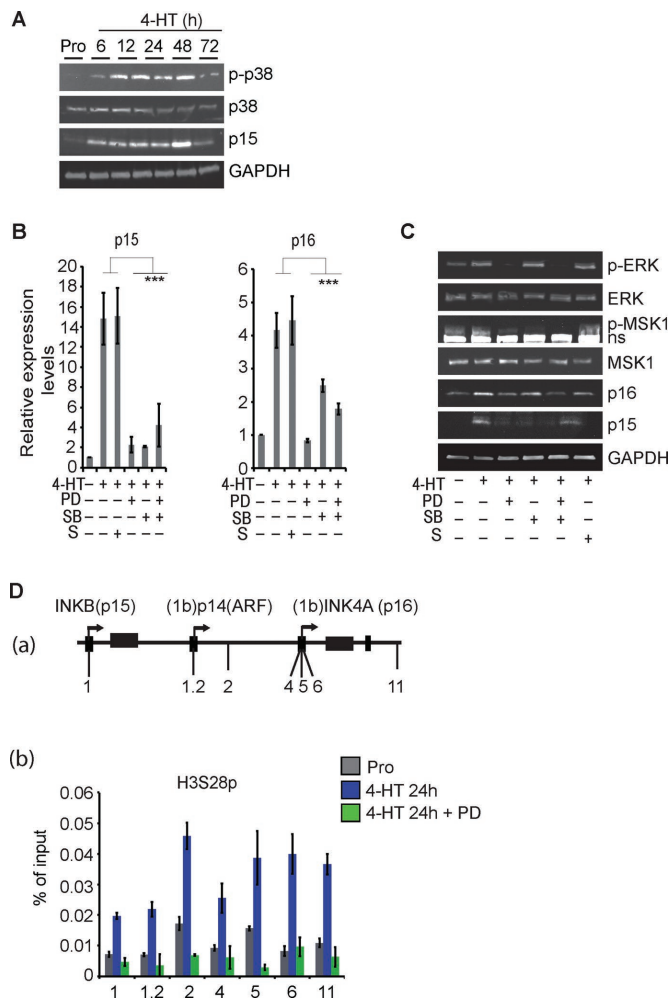
FIGURE 5: MSK1 is regulated by the ERK and p38α pathways in OIS. (A) Western blot analysis of activated phospho-p38 MAP kinase, total p38 MAP kinase, and p15 during senescence induced by 20 nM 4-HT over a 72-h time course for cells growing in 5% oxygen. (B) qRT-PCR analysis of p15INK4B and p16INK4A expression of WI-38hTERT-RAF-ER cells pretreated with SB203580 (SB) and/or PD98059 (PD) or DMSO (S) as indicated for 6 h and then stimulated with 4-HT for 24 h. Data represent the average of three independent biological experiments and are expressed as means ± SD. Student's t test was used to determine statistical significance (***p < 0.0001). (C) WI-38h TERT-RAF-ER cells were pretreated with SB and/or PD or DMSO for 6 h and then stimulated with 4-HT for 24 h. Cell total protein extracts were subjected to Western blotting using antibodies specific for p-MSK1 (S376), MSK1, p-ERK, ERK, p-p38α, and p38α (ns, nonspecific band). (D) (a) Schematic representation of the INK4AB/p14ARF locus, showing the localization of the primer pairs used in ChIP experiments performed in WI-38h TERT RAF1-ER cells; (b) H3S28ph ChIP at the INK4AB/ARF locus. ChIP analysis was performed on chromatin prepared from proliferating cells (Pro), induced to senescence for 24 h, or pretreated with PD98059. The precipitated DNA fragments were subjected to qRT-PCR analysis with selected primers amplifying regions of the INK4AB/p14ARF locus. General IgG was used as a negative control. The values are shown as percentage of input. Data represent the average of three independent biological experiments and are expressed as means ± SD. Statistical analysis of the ChIP experiments is given in Supplemental Table S2.

demethylase JMJD3 is up-regulated in response to an oncogenic stress, recruited to the INK4AB/ARF locus, and implicated in the activation of the locus (Barradas et al., 2009). Studies demonstrated

that PRC2 is unable to bind a H3K27me3 peptide when this peptide is also phosphorylated at S28 and that a H3K27/H3S28 methyl/phospho switch mechanism mediated by the MSK1 kinase regulates gene activation via PRC2 chromatin displacement during neuronal differentiation and mitogenic signaling (Gehani et al., 2010; Lau and Cheung, 2011a). Because Polycomb complexes negatively control the INK4AB/ARF locus in proliferating cells and are rapidly evicted from the locus when cells enter senescence, we wondered whether MSK1 H3 phosphorylation participates in Polycomb complex eviction from the locus and thus contributes to the rapid expression of p15INK4B and p16INK4A in OIS. In the present study, we showed the participation of MSK1 in the activation of the INK4AB/ARF locus in OIS and examined the molecular mechanisms involved in MSK1 activation. We observed that 1) MSK1 is induced and activated during OIS (Figure 1), 2) MSK1 is recruited at the INK4 locus in OIS and phosphorylates H3S28, and 3) the H3S28ph mark correlates with the eviction of Polycomb EZH2 and the transcriptional induction of the locus (Figures 3B and 6). Furthermore, we showed 4) that inhibition of MSK1 by siRNA-mediated knockdown reduces H3S28 phosphorylation at the INK4AB/ARF locus and gene induction (Figure 4) and 5) that, based on ERK and p38 inhibitors, both pathways participate equally in MSK1 activation in OIS (Figure 5). Of interest, we showed that the H3K27me3 mark is still present at the locus, although p15INK4B and p16INK4A genes are strongly expressed 24 h after 4-HT induction, indicating that PcG-target gene derepression is not systematically accompanied by the loss of the H3K27me3 repressive mark. Of interest, it was shown that upon stimulation, the PRC1 target gene ATF3 is expressed despite the presence of the H3K27me3 mark at the promoter (Prickaerts et al., 2012).

Our work shows that the H3K27me3/S28p double mark correlates with PcG protein eviction and transcriptional activation of the INK4 locus. However, based on targeting MSK1 to endogenous Polycomb-silenced genes, it was suggested that H3S28ph is functionally and physically coupled to H3K27Ac (Lau and Cheung, 2011a). This phospho-acetyl mark (H3K27Ac/S28ph) is physically associated with the transcription-initiating (serine 5-phosphorylated) form of RNAP II (Lau and Cheung, 2011a). It was shown that both MSK1 and its homologue, MSK2, coimmunoprecipitate with histone acetyltransferases (HATs), including p300 (Llanos et al., 2009) and CREB-binding protein (CBP; Janknecht, 2003), which are known to acetylate H3 at lysine 27 (Pasini et al., 2010). On the other hand, it was demonstrated that H3 phosphorylation could affect the efficiency of subsequent acetylation reactions (Cheung et al., 2000). However, in our experiments, H3K27Ac enrichment at the locus after RAF1 induction occurred with a 24-h delay compared with the H3S28ph enrichment. Recently it was shown that the treatment of cells with the MSK1 inhibitor H89 impaired the establishment of the H3S28ph mark and the H3Ac mark and the recruitment of MSK1 at the MyoG promoter (Stojic et al., 2011). This indicates a possible link between MSK1, H3S28ph, and H3Ac. In future experiments, it would be interesting to establish which HAT is recruited at the INK4 locus and the role of MSK1 in the dynamic recruitment of this HAT in OIS.

Our results identified a new regulatory pathway for the induction of the INK4 genes based on the sequential activation of MAPKs and p-MSK1. This pathway is a protein phosphorylation cascade with an extensive range of cellular responses. In this study, inhibition of p38 or ERK activity using pharmacological inhibitors blocked RAF1-induced phosphorylation of MSK1 and H3S28ph and also blocked subsequent p16INK4A and p15INK4B expression. The fact that both SB203580 and PD98059 can inhibit expression of p15INK4B and p16INK4A suggests that inhibitors of MAPKs block the phosphorylation of MSK1 at
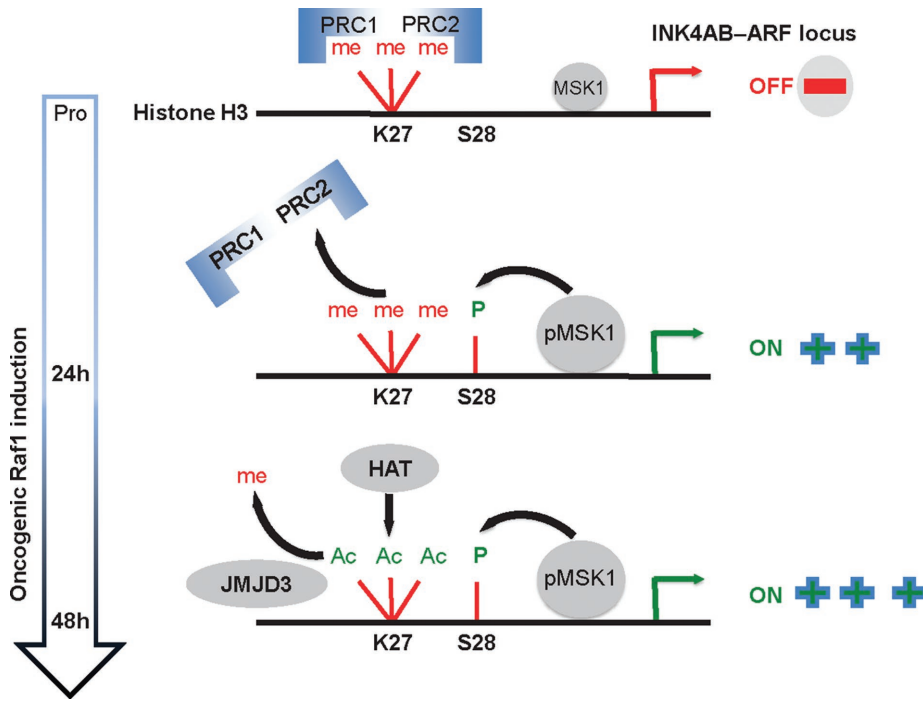
FIGURE 6: MSK1-dependent H3S28 phosphorylation triggers Polycomb eviction and expression of the INK4AB/ARF locus in OIS. 1) The Polycomb proteins (PRC2, PRC1) repress the INK4 locus in proliferating cells. The locus is marked by the repressive H3K7me3 mark. p15^{INK4B} and p16^{INK4A} are repressed: p-MSK1 kinase is constitutively bound to the INK4 locus. 2) A 24-h RAF1 induction provokes increased recruitment/activation of p-MSK1, and H3S28 becomes phosphorylated through the activation of ERK and p38α kinase, leading to the eviction of PcG proteins and derepression of p15^{INK4B} and p16^{INK4A} despite the presence of the H3K27me3 repressive mark. 3) At 48 h after RAF1 induction, the locus loses the repressive mark H3K27me3, indicating that the histone demethylase JMJD3 is active. On recruitment of a H3K27 HAT (not determined), the H3K27Ac mark is enriched at the locus, and transcription is maintained.

distinct additional residues needed for its H3S28 phosphorylation function and that both pathways are needed in OIS. In cells, MSK1 is activated via a complex series of phosphorylation and autophosphorylation reactions downstream of ERK or p38 MAPK, depending on the stimulus used. In addition to being phosphorylated on Thr-581 and Ser-360 by ERK or p38, MSK1 can autophosphorylate on at least six other sites (McCoy et al., 2005). Of them, Thr-700 of MSK1 is phosphorylated by ERK1/2 and p38 (McCoy et al., 2007). It was found that mutation of Thr-700 of MSK1 resulted in a dramatic loss of Thr581 phosphorylation, a site essential for activity (McCoy et al., 2007).

Recently it was found that MSK1 specifically phosphorylates the H3K9me2/1 demethylase p-KDM3A, which then directly interacts with the transcription factor Stat1 to activate p-KDM3A target genes under heat shock conditions (Cheng et al., 2014). It is possible that MSK1 directly phosphorylates JMJD3 to regulate its H3K27me3 demethylase activity/localization at the INK4 locus during OIS. This hypothesis should be tested. In addition, it was demonstrated that the MLL1 complex participates in the activation of the INK4 locus during replicative senescence in mice (Agherbi et al., 2009) and in human cells during the oncogenic checkpoint response. MSK1 might facilitate the activity of JMJD3 and MLL1, both of which are necessary for INK4-ARF activation, (Agger et al., 2009; Kotake et al., 2009), through their recruitment at chromatin.

In conclusion, we show that histone H3S28 phosphorylation through ERK and p38 MAPK activation of MSK1 kinase represents a critical step that links signal transduction pathways that are responsive to external stimuli to help in evicting the Polycomb complexes

that induce INK4AB/ARF gene expression and senescence. Thus our study reveals an important novel mechanism of INK4AB/ARF epigenetic regulation in OIS.

MATERIALS AND METHODS
Cell lines and reagents
WI-38hTERT-RAF-ER cells were maintained in MEM supplemented with glutamine, nonessential amino acids, sodium pyruvate, penicillin–streptomycin, and 10% fetal bovine serum as per the American Type Culture Collection in normoxic (5% O$_2$) culture conditions. For senescence induction, cells were treated with 20 nM 4-HT (Sigma-Aldrich, Lyon, France). Specific inhibitors of p38 and ERK were purchased from Fisher Scientific (Strasbourg, France). Cells were pretreated with PD98059 (50 mM) and SB203580 (10 mM) for 6 h (Pumiglia and Decker, 1997) and stimulated with 4-HT for 24 and 48 h as indicated. Human embryonic fibroblasts WI-38 were grown in DMEM (1 g/l glucose) supplemented with 10% fetal calf serum, 100 U/ml penicillin, 100 µg/ml streptomycin, and 2 mm L-glutamine. Cultures were kept in normoxic (5% O$_2$) culture conditions. Subconfluent cultures were obtained by passaging cells until they entered senescence after ~50 cumulative population doublings (CPDs): early passage, young at passage <25 with <5% of β-gal–positive cells; late passage, senescent at CPD > 45 with 90% of β-gal–positive cells.

For construction of the BJ BRAFV600E cells, a DNA fragment encoding B-RAF-V600E with three tandem hemagglutinin (HA) epitope tags at the N-terminus was synthesized with AgeI + MluI restriction sites. This fragment was substituted for the AgeI + MluI fragment of the pTRIPz lentiviral vector. The resulting lentiviral plasmid places the 3HA-B-RAF-V600E sequence under the control of a tet-ON promoter. Amphotropic lentivirus was produced by transient transfection of 293T cells with the appropriate packaging plasmids and used to infect BJ/hTERT (hygromycin-resistant) human foreskin fibroblasts (Takara Bio USA) in an L3 confinement laboratory. Infected cells were selected for their resistance to puromycin conferred by the pTRIPz vector. After verification that the infected cells did not produce infectious viral particles, the cells were transferred to an L2 facility. Addition of doxycycline (25 ng/ml) leads to expression of 3HA-B-RAF-600E and rapid induction of cellular senescence.

Quantification of mRNA levels by qRT-PCR
RNA was purified using the RNeasy Plus Mini Kit (74134; Qiagen, Germany), and cDNA was generated by RT-PCR using Applied Biosystems TaqMan Reverse Transcription Reagents. qPCR analysis was performed on a CFX96 real-time system device (Bio-Rad, Hercules, CA) using IQ SYBR Supermix (Bio-Rad) according to the manufacturer's instructions. All samples were analyzed in triplicate. U6 RNA was used as an endogenous control. The average and SDs of three biological replicates were obtained and assessed for significance using an unpaired Student's t test. For all experiments, ***p < 0.0001,

siRNA transfection of WI-38hTERT/GFP- RAF1-ER cells

Proliferating WI-38h TERT/GFP-RAF1-ER cells were transfected at 50% confluency with Dharmafect 4 transfection reagent (Thermo-Fisher Scientific, Surrey, United Kingdom). At 48 h after transfection, cells were induced to senesce with 4-HT and collected at the indicated time points. All siRNAs were used at a final concentration of 20 nM. MSK1 siRNAs and nonsilencing controls are from Ambion Silencer Select siRNA (s17691 and s17692).

MSK1 transfection

The pCMV5-Flag vector (Vec) and pCMV5-Flag–wild-type MSK1 (MSK1; generous gifts from D. R. Alessi, Medical Research Council Protein Phosphorylation Unit, Department of Biochemistry, University of Dundee, Dundee, Scotland) and WI-38hTERT-RAF-ER cells were cultured on 96-well plates, transfected with the pCMV5 vector encoding the Flag-epitope–tagged MSK1 constructs using Turbofect reagent (Thermo Scientific), and then left unstimulated. Transfection efficiency was controlled in indirect immunofluorescence using a Flag antibody (F7425; Sigma-Aldrich). An average of 60% transfection efficiency was achieved. At 48 h posttransfection, the cells were fixed and stained as previously described (Agherbi et al., 2009). Cells were washed 3 × 5 min with cold phosphate-buffered saline (PBS) and stored in PBS at 4°C until images were collected.

Immunofluorescence

Cells seeded on glass coverslip were fixed in 4% paraformaldehyde for 15 min, washed in PBS, permeabilized with 0.5% Triton X-100 for 10 min, and incubated in blocking buffer (PBS, 3% bovine serum albumin) for 1 h at room temperature. Primary antibodies were incubated at 37°C for 1 h. The secondary antibodies (Alexa Fluor 594) were incubated at 1:2000 at 37°C for 1 h, followed by 4′,6-diamidino-2-phenylindole (DAPI) incubation at 0.2 μg/ml for 10 min. The concentrations of the antibodies were 1:250 for anti-pMSK1 and p-H3S28, 1:500 for MSK1, and 1:500 for EZH2. Image capture was performed on slides mounted with Prolong Gold (Invitrogen, Thermo Fisher Scientific, Villebon sur Yvette, France). Images were collected with a microscope (DM5000; Leica) equipped with a charge-coupled device (CCD) camera (CoolSNAP ES; Roper Scientific, Munich, Germany), a 40× objective, Semrock filters, and the acquisition software MetaMorph (Molecular Devices). Image processing (adjust contrast) and quantification were done by the ImageJ software. Statistical analysis of MSK1, p-MSK1, and H3S28ph accumulation in cell nuclei in proliferation 24 and 48 h after senescence induction was assessed by the Wilcoxon–Mann–Whitney test.

Senescence-associated β-galactosidase

Cells were stained as previously described (Agherbi et al., 2009). Cells were washed 3 × 5 min with cold PBS and stored in PBS at 4°C until images were collected. Expression of SA β-gal–positive cells was enumerated using an inverted microscope and compared with the total number of cells. At least 100 cells/well in three random fields were counted in triplicate wells.

Chromatin immunoprecipitation

ChIP was performed using the Magna ChIP Kit (Millipore, Molsheim, France) with some modifications. Briefly, 2 × 10^6 cells (4-HT treated or untreated) were lysed in the Magna ChIP Cell Lysis Buffer at 4°C and nuclei sonicated for 18 min (45 s on, 45 s off with the Diagenode [Seraing, Belgium] Bioruptor) to yield 300– to 600–base pair DNA

fragments. Sonicated chromatin from 2 × 10^6 cells was immunoprecipitated overnight in Magna ChIP Kit Dilution Buffer at 4°C with 3 μg of the indicated antibodies or a nonspecific antibody as a control (Supplemental Table S1). Washes, proteinase K treatment, and reverse cross-link were done as in the Magna ChIP Kit (Millipore) protocol. DNA was purified using Millipore spin columns. Input DNA was analyzed simultaneously for normalization. As a control, total H3 ChIP experiments were done with proliferating and senescent cells. qPCR analysis using the INK4 primers did not show any difference in these two conditions (unpublished data). All primers used are listed in Supplemental Table S1. The average and SDs of three biological replicates were obtained and assessed for significance using an unpaired Student's t test. Statistical analysis of ChIP experiments are listed in Supplemental Table S2.

Western blots

Whole-cell protein extracts were prepared in 1% SDS, 1 mM sodium vanadate, 10 mM Tris, pH 7.4, 1% Triton, and 0.5 M NaCl supplemented with protease inhibitors and phosphatase inhibitors (Sigma-Aldrich) with sonication until the viscosity of the sample was reduced. Protein concentration was determined using the Bradford assay (Bio-Rad). Western blots were performed using standard procedures (primary antibody dilutions of 1:1000 except for the glyceraldehyde-3-phosphate dehydrogenase [GAPDH] antibody, which was diluted at 1:5000 (Supplemental Table S1 lists the antibodies used in this study). For chromatin isolation for Western blots, cells were cross-linked using 1% formaldehyde for 10 min. The cytosolic fraction was separated from nuclei by centrifugation for 5 min at 4°C at 800 × g. The nuclear pellet was incubated in a nuclear lysis buffer (Millipore), briefly sonicated at 4°C, and centrifuged at 10,000 rpm. The resulting chromatin-associated protein fraction was reverse cross-linked at 62°C for 2 h, treated with DNase for 15 min, and analyzed by Western blotting as described. We used 10% Tris-glycine and 4%–12% (Bio-Rad) to separate the proteins. Prestained protein ladder (Thermo Fisher) was used as a molecular weight marker. Western blots were visualized using a CCD camera (G-Box Ozyme).

REFERENCES

Agger K, Cloos PA, Rudkjaer L, Williams K, Andersen G, Christensen J, Helin K (2009). The H3K27me3 demethylase JMJD3 contributes to the activation of the INK4A-ARF locus in response to oncogene- and stress-induced senescence. Genes Dev 23, 1171–1176.

Agherbi H, Gaussmann-Wenger A, Verthuy C, Chasson L, Serrano M, Djabali M (2009). Polycomb mediated epigenetic silencing and replication timing at the INK4a/ARF locus during senescence. PLoS One 4, e5622.

Barradas M, Anderton E, Acosta JC, Li S, Banito A, Rodriguez-Niedenfuhr M, Maertens G, Banck M, Zhou MM, Walsh MJ, et al. (2009). Histone demethylase JMJD3 contributes to epigenetic control of INK4a/ARF by oncogenic RAS. Genes Dev 23, 1177–1182.

Bracken AP, Kleine-Kohlbrecher D, Dietrich N, Pasini D, Gargiulo G, Beekman C, Theilgaard-Monch K, Minucci S, Porse BT, Marine JC, et al. (2007). The Polycomb group proteins bind throughout the INK4A-ARF locus and are disassociated in senescent cells. Genes Dev 21, 525–530.

Cao R, Wang L, Wang H, Xia L, Erdjument-Bromage H, Tempst P, Jones RS, Zhang Y (2002). Role of histone H3 lysine 27 methylation in Polycomb-group silencing. Science 298, 1039–1043.

Cao R, Zhang Y (2004). The functions of E(Z)/EZH2-mediated methylation of lysine 27 in histone H3. Curr Opin Genet Dev 14, 155–164.

Cheng MB, Zhang Y, Cao CY, Zhang WL, Zhang Y, Shen YF (2014). Specific phosphorylation of histone demethylase KDM3A determines target gene expression in response to heat shock. PLoS Biol 12, e1002026.

Cheung P, Tanner KG, Cheung WL, Sassone-Corsi P, Denu JM, Allis CD (2000). Synergistic coupling of histone H3 phosphorylation and acetylation in response to epidermal growth factor stimulation. Mol Cell 5, 905–915.

Collado M, Blasco MA, Serrano M (2007). Cellular senescence in cancer and aging. Cell 130, 223–233.

Courtois-Cox S, Jones SL, Cichowski K (2008). Many roads lead to oncogene-induced senescence. Oncogene 27, 2801–2809.

Davie JR (2003). MSK1 and MSK2 mediate mitogen- and stress-induced phosphorylation of histone H3: a controversy resolved. Sci STKE 2003, PE33.

Deak M, Clifton AD, Lucocq LM, Alessi DR (1998). Mitogen- and stress-activated protein kinase-1 (MSK1) is directly activated by MAPK and SAPK2/p38, and may mediate activation of CREB. EMBO J 17, 4426–4441.

Drobic B, Perez-Cadahia B, Yu J, Kung SK, Davie JR (2010). Promoter chromatin remodeling of immediate-early genes is mediated through H3 phosphorylation at either serine 28 or 10 by the MSK1 multi-protein complex. Nucleic Acids Res 38, 3196–3208.

Dyson MH, Thomson S, Inagaki M, Goto H, Arthur SJ, Nightingale K, Iborra FJ, Mahadevan LC (2005). MAP kinase-mediated phosphorylation of distinct pools of histone H3 at S10 or S28 via mitogen- and stress-activated kinase 1/2. J Cell Sci 118, 2247–2259.

Gehani SS, Agrawal-Singh S, Dietrich N, Christophersen NS, Helin K, Hansen K (2010). Polycomb group protein displacement and gene activation through MSK-dependent H3K27me3S28 phosphorylation. Mol Cell 39, 886–900.

Janknecht R (2003). Regulation of the ER81 transcription factor and its coactivators by mitogen- and stress-activated protein kinase 1 (MSK1). Oncogene 22, 746–755.

Jeanblanc M, Ragu S, Gey C, Contrepois K, Courbeyrette R, Thuret JY, Mann C (2012). Parallel pathways in RAF-induced senescence and conditions for its reversion. Oncogene 31, 3072–3085.

Kotake Y, Zeng Y, Xiong Y (2009). DDB1-CUL4 and MLL1 mediate oncogene-induced p16INK4a activation. Cancer Res 69, 1809–1814.

Lau PN, Cheung P (2011a). Histone code pathway involving H3 S28 phosphorylation and K27 acetylation activates transcription and antagonizes polycomb silencing. Proc Natl Acad Sci USA 108, 2801–2806.

Lau PN, Cheung P (2011b). Unlocking polycomb silencing through histone H3 phosphorylation. Cell Cycle 10, 1514–1515.

Llanos S, Cuadrado A, Serrano M (2009). MSK2 inhibits p53 activity in the absence of stress. Sci Signal 2, ra57.

McCoy CE, Campbell DG, Deak M, Bloomberg GB, Arthur JS (2005). MSK1 activity is controlled by multiple phosphorylation sites. Biochem J 387, 507–517.

McCoy CE, Macdonald A, Morrice NA, Campbell DG, Deak M, Toth R, McIlrath J, Arthur JS (2007). Identification of novel phosphorylation sites in MSK1 by precursor ion scanning MS. Biochem J 402, 491–501.

Michaloglou C, Vredeveld LC, Soengas MS, Denoyelle C, Kuilman T, van der Horst CM, Majoor DM, Shay JW, Mooi WJ, Peeper DS (2005). BRAFE600-associated senescence-like cell cycle arrest of human naevi. Nature 436, 720–724.

Narita M, Nunez S, Heard E, Narita M, Lin AW, Hearn SA, Spector DL, Hannon GJ, Lowe SW (2003). Rb-mediated heterochromatin formation and silencing of E2F target genes during cellular senescence. Cell 113, 703–716.

Pasini D, Malatesta M, Jung HR, Walfridsson J, Willer A, Olsson L, Skotte J, Wutz A, Porse B, Jensen ON, et al. (2010). Characterization of an antagonistic switch between histone H3 lysine 27 methylation and acetylation in the transcriptional regulation of Polycomb group target genes. Nucleic Acids Res 38, 4958–4969.

Perez-Cadahia B, Drobic B, Davie JR (2011). Activation and function of immediate-early genes in the nervous system. Biochem Cell Biol 89, 61–73.

Prickaerts P, Niessen HE, Mouchel-Vielh E, Dahlmans VE, van den Akker GG, Geijselaers C, Adriaens ME, Spaapen F, Takihara Y, Rapp UR, et al. (2012). MK3 controls Polycomb target gene expression via negative feedback on ERK. Epigenetics Chromatin 5, 12.

Pumiglia KM, Decker SJ (1997). Cell cycle arrest mediated by the MEK/mitogen-activated protein kinase pathway. Proc Natl Acad Sci USA 94, 448–452.

Serrano M (2007). Cancer regression by senescence. N Engl J Med 356, 1996–1997.

Stojic L, Jasencakova Z, Prezioso C, Stutzer A, Bodega B, Pasini D, Klingberg R, Mozzetta C, Margueron R, Puri PL, et al. (2011). Chromatin regulated interchange between polycomb repressive complex 2 (PRC2)-Ezh2 and PRC2-Ezh1 complexes controls myogenin activation in skeletal muscle cells. Epigenetics Chromatin 4, 16.

Takahashi A, Ohtani N, Yamakoshi K, Iida S, Tahara H, Nakayama K, Nakayama KI, Ide T, Saya H, Hara E (2006). Mitogenic signalling and the p16INK4a-Rb pathway cooperate to enforce irreversible cellular senescence. Nat Cell Biol 8, 1291–1297.

Wang W, Chen JX, Liao R, Deng Q, Zhou JJ, Huang S, Sun P (2002). Sequential activation of the MEK-extracellular signal-regulated kinase and MKK3/6-p38 mitogen-activated protein kinase pathways mediates oncogenic ras-induced premature senescence. Mol Cell Biol 22, 3389–3403.

Zhang R, Chen W, Adams PD (2007). Molecular dissection of formation of senescence-associated heterochromatin foci. Mol Cell Biol 27, 2343–2358.